Representative elementary volume (REV) of cementitious materials from three-dimensional pore structure analysis

M.H.N. Yio, H.S. Wong*, N.R. Buenfeld

Concrete Durability Group, Department of Civil and Environmental Engineering, Imperial College London, SW7 2AZ, UK

A B S T R A C T

The representative elementary volume (REV) is a fundamental property of a material, but no direct measurements exist for cementitious materials. In this paper, the REV of cement pastes with supplementary cementitious materials (GGBS, PFA, SF) was determined by analysing the three-dimensional pore structure ($> 0.2\,\mu m$) using laser scanning confocal microscopy (LSCM). The effect of axial distortion inherent to LSCM on 3D pore structure was also investigated. A range of 3D pore parameters was measured using skeletonisation, maximal ball and random walker algorithms. Results show that axial distortion has insignificant effects on most parameters except Euler connectivity, average pore and throat volumes and directional diffusion tortuosities. Most pore parameters become independent of sampling volume at $\approx 60^3\,\mu m^3$ except diffusion tortuosities and formation factor. The REV for porosity calculated based on a statistical approach at eight realisations and 5% relative error was found to be $\approx 100^3\,\mu m^3$.

1. Introduction

Representative elementary volume (REV), also known as representative volume element (RVE), is an important parameter for understanding and modelling the properties of multi-scale composite materials such as cement-based materials. The REV is the smallest volume over which a measurement or simulation can be carried out to produce a result that is representative of the macroscopic property. This is important because it is often difficult/impractical to experimentally capture or computationally generate composite materials at full length scales. Several definitions of REV exist, but there are two common requirements [1]: (1) the REV must be of the right size to contain sufficient microstructural features to depict the macroscopic property representatively, and (2) the REV is determined for a specified property and it is essentially independent of the sampling position within the material. Bear [2] presented the concept of REV graphically as shown in Fig. 1. The fluctuations in the property of interest (e.g. porosity) reduce with increasing sampling volume and the volume at which fluctuations become insignificant is taken as the REV. For an inhomogeneous medium however, the property may gradually change again as the sampling volume increases further.

The REV depends on the length scale of the features of interest. Cement-based materials contain features ranging from nanoscale gel pores and hydrates to microscale capillary pores and millimetre-sized air voids and aggregate particles. Determining the REV at the concrete scale is relatively straightforward because one could simply carry out measurements on samples of varying sizes. However, it is much more challenging to do this at the scale of capillary pores. Yet, this is important because of its relevance to mass transport processes. The REV at the capillary pore scale is generally considered to be $100^3\,\mu m^3$. However, this value was derived from numerical modelling of computer generated 3D pore structures [3–5]. For example, Zhang et al. [4] adopted a numerical-statistical approach to determine the REV based on finite element simulated diffusion of tritiated water through 3D models of cement pastes (w/c 0.30 to 0.60) generated with HYMOS-TRUC3D. Later, Ukrainczyk and Koenders [5] found that the REV of computer generated 3D pore structures is highly dependent on the employed numerical resolution, boundary conditions, initial particle size distribution of anhydrous cement particles and degree of hydration.

To the best of our knowledge, the REV for cementitious materials has never been measured experimentally at the capillary pore scale. This could be partly due to lack of suitable experimental techniques to characterise the 3D characteristics of pore structure at sufficiently high resolution. Recently, a new 3D imaging approach which combines laser scanning confocal microscopy (LSCM) with serial sectioning [6] has enabled 3D reconstruction of pore structure at submicron spatial resolution. The method involves stitching of sequential confocal stacks based on phase correlation and so is able to image large volumes without resolution loss. Therefore, the method not only lends itself well for 3D pore characterisation, but also opens up possibilities for determining the REV of cement-based materials.

A number of issues need to be addressed to achieve this. For example, accurate segmentation of the pore structure from LSCM images is a prerequisite for successful analyses, but this is particularly
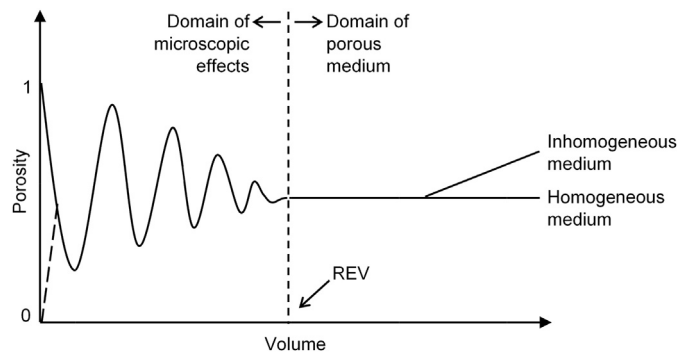

Fig. 1. Change in property of interest (e.g. porosity) as a function of sample volume to define REV (after Bear [2]).

challenging due to the complex boundaries between pores and solid hydration products. Uneven brightness that may occur along the depth of the reconstructed image further complicates the segmentation process. Fredrich [7] segmented the pore structure of Berea stone from 3D LSCM images using the local minima between solid and pore peaks in the image histogram as a threshold. Oh and Lindquist [8] have further developed a kriging-based method that determines the threshold based on minimum variance estimation within a pre-assigned threshold range, which also lies between the solid and pore peaks. However, the determination is not straightforward and is usually user-specified. Both methods are not applicable to this study because LSCM images of cement-based materials do not exhibit bimodal distribution in the histogram. Other approaches such as iterative k-means clustering also require an a priori threshold to be estimated [9].

Furthermore, the process for quantitative analysis of the 3D pore structure based on images reconstructed by such a method has not been established to date. It is also well recognised that 3D LSCM images suffer from distortion in the optical (axial) axis because of two main reasons [10,11]. First, the resolution is inherently anisotropic along the optical axis due to the elongation of point spread function (PSF). Second, mismatch of refractive indices between the immersion medium and the sample or within the sample itself can lead to severe spherical aberrations. Such distortions can produce misleading results when volumetric measurements are made. In biological imaging, the axial distortion caused by refractive index mismatch can be corrected empirically by inserting fluorescent microspheres of known geometries into the specimen to measure the elongation [12,13]. However, this approach is unsuitable for hardened cement-based materials. While it may

be possible to place 'micro-standards' in the fresh mix, they will either end up in the pore space or be engulfed by hydration products and therefore cannot be distinguished in hardened cement paste. Depending on the size of the standards, the resulting microstructure may also be altered owing to the formation of new interfaces. Moreover, these standards are required in large quantities and dispersed within the system to ensure a homogeneous correction.

The main aim of this paper is to: (1) study the effects of axial distortion in LSCM images on 3D pore parameters, and (2) estimate the REV for different pore parameters and cementitious systems. A method for pore segmentation and protocol for charactering the 3D pore structure was first developed. Then, the methods were validated on measurements of ideal 3D model structures. Finally, the methods were applied to quantify over twenty 3D pore structure of real cementitious samples in order to study the effects of axial distortion and to determine the REV. A range of blended cement pastes containing CEM I, silica fume, pulverised fuel ash and ground granulated blastfurnace slag cured to 7 and 90 days were tested.

2. Experimental

2.1. Materials and sample preparation

Four cement pastes containing CEM I and CEM I blended with silica fume (SF), pulverised fuel ash (PFA) or ground granulated blastfurnace slag (GGBS) were prepared and cured for 7 and 90 days to produce samples with a range of microstructure. Mix proportions are shown in Table 1. The oxide compositions and properties of the cementitious materials are given in Table 2. The Bogue composition of CEM I was 53.1% C_3S, 19.1% C_2S, 10.8% C_3A and 7.2% C_4AF. The fineness and specific gravity of the CEM I were 291 m^2/kg and 3.06 respectively.

All wet-mixing was done in a Hobart mixer for 4 min. PFA and GGBS were dry-mixed with CEM I for 1 min before water was added. For the mix with SF, a polycarboxylate-based superplasticiser was added to the water at 0.4 wt% binder and pre-mixed with SF for 1 min to disperse agglomerated particles. All mixes were cast in steel moulds of 100 mm diameter × 25 mm height and compacted in two layers using a vibrating table. Immediately after casting, the samples were covered with plastic sheets and wet hessian to prevent loss of moisture, and left to harden at 20 °C. After 24 h, the samples were demoulded and cured in a fog room at 100% RH and 20 °C for 7 and 90 days.

For each mix and curing age, four replicate discs were prepared; one for LSCM imaging and three for mass transport measurements, the latter will be reported in a separate publication. A slight amount of bleeding was observed after casting therefore two additional disc

Table 1
Mix proportions.

Sample ID	CEM I (kg/m³)	SCM (wt% total binder)	SF (kg/m³)	PFA (kg/m³)	GGBS (kg/m³)	Water (kg/m³)	Total w/b	Free w/b[a]
P0.45	1290	–	–	–	–	581	0.45	0.426
P0.45 SF	1158	9	115	–	–	573	0.45	0.445
P0.45 PFA	965	23	–	288	–	564	0.45	0.434
P0.45 GGBS	505	60	–	–	758	568	0.45	0.415

[a] After correcting for water lost to bleeding.

Table 2
Oxide compositions and properties of cementitious materials used.

Binder	Oxide composition (wt%)									LOI (%)	Laser granulometry d_{50} (µm)
	CaO	SiO₂	Al₂O₃	Fe₂O₃	MgO	Na₂O$_{(eq)}$	K₂O	SO₃	Cl⁻		
CEM I	63.4	20.8	5.4	2.4	1.5	0.3	0.7	2.9	< 0.1	2.10	N/A
SF	0.2	98.6	0.3	0.0	0.1	0.2	–	0.1	–	N/A	0.25
PFA	0.1	72.2	24.3	0.4	0.1	0.3	–	0.1	–	N/A	7.00
GGBS	40.8	36.5	11.6	1.4	7.5	0.5	–	2.1	–	− 0.99	8.00